Pharmaceutical Research, Vol. 26, No. 5, May 2009 (© 2009)
DOI: 10.1007/s11095-008-9823-9

Research Paper

Relative Importance of Intestinal and Hepatic Glucuronidation—Impact on the Prediction of Drug Clearance

Helen E. Cubitt,[1] J. Brian Houston,[1] and Aleksandra Galetin[1,2]

Received November 6, 2008; accepted December 29, 2008; published online January 31, 2009

Purpose. To assess the extent of intestinal and hepatic glucuronidation *in vitro* and resulting implications on glucuronidation clearance prediction.
Methods. Alamethicin activated human intestinal (HIM) and hepatic (HLM) microsomes were used to obtain intrinsic glucuronidation clearance ($CL_{int,UGT}$) for nine drugs using substrate depletion. The *in vitro* extent of glucuronidation (fm_{UGT}) was determined using P450 and UGT cofactors. Utility of hepatic CL_{int} for the prediction of *in vivo* clearance was assessed.
Results. fm_{UGT} (8–100%) was comparable between HLM and HIM with the exception of troglitazone, where a nine-fold difference was observed (8% and 74%, respectively). Scaled intestinal $CL_{int,UGT}$ (per g tissue) was six- and nine-fold higher than hepatic for raloxifene and troglitazone, respectively, and comparable to hepatic for naloxone. The remaining drugs had a higher hepatic than intestinal $CL_{int,UGT}$ (average five-fold). For all drugs with P450 clearance, hepatic $CL_{int,CYP}$ was higher than intestinal (average 15-fold). Hepatic $CL_{int,UGT}$ predicted on average 22% of observed *in vivo* CL_{int}; with the exception of raloxifene and troglitazone, where the prediction was only 3%.
Conclusion. Intestinal glucuronidation should be incorporated into clearance prediction, especially for compounds metabolised by intestine specific UGTs. Alamethicin activated microsomes are useful for the assessment of intestinal glucuronidation and fm_{UGT} *in vitro*.

KEY WORDS: clearance prediction; glucuronidation; intestine.

Uridine Diphosphate Glucuronosyltransferases (UGTs) catalyse glucuronidation, the conjugation reaction that together with Cytochrome P450 (P450) reactions, accounts for most of the drug metabolism that occurs in the liver (1). There is an increasing awareness of the importance of glucuronidation, especially in drug development (2). Therefore, there is a need to develop methods to predict *in vivo* glucuronidation clearance from *in vitro* data to the same level attained for P450 enzymes (3–8).

Although glucuronidation has been investigated in a range of *in vitro* systems, there has been little attention paid to the prediction of UGT clearance, compared to the extensive work already documented for P450s. Drug clearance predictions using microsomal data have tended to under-predict *in vivo* clearance (1,9–11), leading to a concern over the validity of their use in glucuronidation studies (12). Although both UGT and P450 enzymes are membrane bound in the endoplasmic reticulum, the UGT active site faces the lumen, resulting in latency in microsomal preparations, probably due to a diffusional barrier for substrate and cofactor access. Several methods have been introduced to circumvent this problem, including the use of the pore-forming agent alamethicin or a detergent or sonication treatment (13,14). Numerous other incubation conditions have been reported to influence glucuronidation activity, namely pH and the concentrations of saccharic acid lactone and EDTA (1,15).

An additional factor that may contribute to the observed under-prediction trend of glucuronidation clearance, is the extent of intestinal metabolism, which is generally omitted from the *in vitro–in vivo* scaling strategy (16). The human small intestine expresses a range of P450 enzymes, with CYP3A4 accounting for ~80% of the total P450 protein content (17). Although the total amount of CYP3A expressed in the human small intestine represents only ~1% of the hepatic estimate, the metabolic activities of liver and intestinal P450s are comparable once normalised for the mean population relative abundance of these enzymes (18). The human intestine also expresses a range of UGTs, including UGT1A1 and UGT2B7 (as in the liver), and the intestine specific enzymes, UGT1A7, UGT1A8 and UGT1A10 (19). UGTs are thought to have an analogous regional distribution in the intestine to P450s (20), with the highest levels found in the proximal regions and in mature enterocytes lining the villus tips. However, the relative UGT expression levels *in vivo* are still not

[1] School of Pharmacy and Pharmaceutical Sciences, University of Manchester, Stopford Building Oxford Road, Manchester, M13 9PT, UK.
[2] To whom correspondence should be addressed. (e-mail: Aleksandra.Galetin@manchester.ac.uk)

ABBREVIATIONS: CL_{int}, intrinsic clearance; $CL_{int,u}$, intrinsic clearance corrected for non-specific protein binding; $CL_{int,UGT}$, intrinsic clearance by glucuronidation; $CL_{int,CYP}$, intrinsic clearance by cytochrome P450 metabolism; fm_{UGT}, fraction metabolised by glucuronidation; fu_{inc}, fraction unbound from protein in the incubation; fu_b, fraction unbound in the blood; fu_p, fraction unbound in the plasma; HIM, human intestinal microsomes; HLM, human liver microsomes; rmse, root mean squared error; R_B, blood to plasma concentration ratio; UGT, uridine diphosphate glucuronosyltransferase.

clearly defined. A recent study by Cao *et al.* (21) indicated a three-fold greater expression of UGTs relative to CYP3A4 in the human duodenum, but it is questionable whether this estimate will reflect the UGT: P450 abundance ratio along the whole length of the gut.

Several studies have assessed the catalytic activity of intestinal UGT enzymes in comparison to the liver (22–26). However, variability in the segment of the gut used (duodenum or jejunum) (10,26) and differential methods used for UGT activation (10,27) or preparation method for intestinal microsomes (mucosal scraping or enterocyte elution) makes an unequivocal comparison difficult. A recent systematic comparison of the metabolic activity of intestinal and hepatic P450 enzymes has shown that the enterocyte elution method for preparation of intestinal microsomes results in a higher activity of intestinal metabolic enzymes in comparison to mucosal scraping (18).

The aim of the current study was to assess intestinal and hepatic glucuronidation clearance for nine substrates, selected on the basis of their differing enzyme specificities, using standardised *in vitro* conditions. *In vitro* intrinsic clearance was obtained in alamethicin activated human intestinal (HIM) and hepatic (HLM) microsomes using a substrate depletion approach at low substrate concentration. The *in vitro* extent of glucuronidation (fm_{UGT}) was determined in both liver and intestine using separate incubations with either NADPH (P450) or UDPGA (UGT) cofactors. The importance of intestinal relative to hepatic glucuronidation and the implications on clearance prediction are discussed.

MATERIALS AND METHODS

Chemicals. All solvents were purchased from VWR International (Lutterworth, UK). All other compounds and reagants were purchased from Sigma-Aldrich Company Ltd (Dorset, UK).

Source of the Microsomes. Pooled HLM (A, $n=30$) were used for all nine drugs and were purchased from BD Gentest (Woburn, MA). Glucuronidation clearance for raloxifene and troglitazone was assessed further in two additional pools of HLM. (B, $n=22$ and C, $n=33$). The range of enzyme activity across the three pools of HLM was 730–1,000pmol/mg/min and 250–330pmol/mg/min for UGT1A1 and total CYP activity, respectively. Pooled HIM ($n=10$) prepared by enterocyte elution mainly of the jejunum section were purchased from Xenotech, LLC (Kansas, USA). The UGT (4-methylumbelliferone) and CYP3A4 (testosterone 6β-hydroxylation) activity in HIM was 8.05 nmol/mg/min and 1,510 pmol/mg/min, respectively.

Microsomal Incubations. All microsomes were stored at −80°C and rapidly thawed just before use at 37°C. Incubations for all nine compounds were carried out in duplicate using an Eppendorf thermomixer (Hamburg, Germany) at 37°C and 1,400 rpm. Activation of microsomal protein by alamethicin was performed as described previously (13,14). Alamethicin was incubated at 50 μg/mg microsomal protein for 15 min on ice. All substrates were preincubated on the thermomixer for 5 min at 37°C with activated protein (HLM or HIM) and either UGT (0.1 M phosphate buffer pH 7.1 containing 3.45 mM magnesium chloride, 1.15 mM EDTA and 115 μM saccharic acid lactone monohydrate) or P450 (0.1 M phosphate buffer pH 7.4) phosphate buffer. Reactions were initiated by the addition of either UGT (5 mM UDPGA) or P450 (a NADPH regenerating system containing 1 mM $NADP^+$, 7.5 mM isocitric acid, 10 mM magnesium chloride, 1.2 unit of isocitric dehydrogenase) cofactor, to give a final incubation volume of 800 μl. Substrate concentrations for eight of the nine compounds in the final incubation was 1 μM; the exception being mycophenolic acid, which was used at a concentration of 10 μM. The final concentration of organic solvent in the incubation media was 0.1%. Microsomal protein concentrations in the incubations for seven of the nine compounds (buprenorphine, diclofenac, gemfibrozil, mycophenolic acid, naloxone, salbutamol and troglitazone) were 0.5 mg/ml for HLM and 1 mg/ml for HIM. However, for quercetin and raloxifene, a much lower protein concentration was needed of 0.1 mg/ml for both HLM and HIM. Control incubations were also performed for each drug with no cofactor present, showing no clearance. At each time point, 100 μl of the incubation was removed and the reaction terminated by the addition of 100 μl of ice-cold acetonitrile containing the internal standard as specified in Table I. The total length of the incubations was 60 min for buprenorphine, mycophenolic acid, naloxone, salbutamol and troglitazone; 50 min for gemfibrozil and diclofenac; 30 min for raloxifene and 10 min for quercetin. Samples were centrifuged at 1,400 *g* (MSE Mistral 3000i centrifuge, London, UK) for 10 min, and the parent compound in an aliquot (10 μl) of the supernatant was analysed by LC-MS/MS.

Determination of Experimental fu_{inc}. The fu_{inc} values for all compounds except quercetin were experimentally determined in HLM at protein concentrations of 0.1, 0.5 and 1 mg/ml using the high-throughput dialysis method as described previously (28). Dialysis membranes had a 12 to 14 kDa molecular mass cutoff and were purchased from

Table I. Experimental Conditions for the Selected Compounds with Details on the Internal Standards, Mass Transitions and Retention Times

Compound	Internal standard	Electrospray ionisation	Transition	Cone voltage (V)	Collision voltage (eV)	Retention time (min)
Buprenorphine	Mibefradil	Positive	468.5>396.3	85	50	2.7
Diclofenac	Tolbutamide	Negative	293.9>250.1	50	11	4.6
Gemfibrozil	Tolbutamide	Negative	249.2>121.2	75	10	4.5
Mycophenolic acid	Warfarin	Negative	319.4>191.2	90	24	4.0
Naloxone	Levallorphan	Positive	328.4>310.3	51	25	3.0
Quercetin	Desipramine	Positive	303.3>229.3	110	30	2.9
Raloxifene	Terfenadine	Positive	474.4>112.3	100	20	3.3
Salbutamol	Propanolol	Positive	240.4>148.4	18	17	2.3
Troglitazone	Diltiazem	Positive	442.4>165.4	65	30	3.3

HTDialysis, LLC (Gales Ferry, CT). The drugs were added to the acceptor chamber with 0.1 M phosphate buffer at a concentration of 1 μM except mycophenolic acid, which was used at a concentration of 10 μM. The fu_{inc} values for quercetin were predicted using an algorithm proposed by Hallifax and Houston (29), due to compound degradation during equilibrium dialysis.

LC-MS/MS. The LC-MS/MS system used consisted of a Waters 2790 with a Micromass Quatro Ultima triple quadruple mass spectrometer (Waters, Elstree, UK). Varying gradients of four mobile phases were used, the compositions of which were (1) 90% water and 0.05% formic acid with 10% acetonitrile (2) 10% water and 0.05% formic acid with 90% acetonitrile (3) 90% water and 10 mM ammonium acetate with 10% acetonitrile (4) 10% water and 10 mM ammonium acetate with 90% acetonitrile. A Luna C18 column 3 μm, 50×4.6 mm (Phenomenex, Macclesfield, UK) was used for chromatographic separation of analytes. The flow rate was 1 ml/min, and this was split to 0.25 ml/min before entering the mass spectrometer. Further analytical parameters are described in Table I. The ion chromatograms were integrated and quantified using Micromass QuanLynx software (Waters, Elstree, UK).

Data Analysis. Data from the mean of two incubations were analysed using a nonlinear single exponential fit and the elimination rate constant (k) was determined using Grafit 5 (Erithacus Software, Horley, UK). The half-life ($t_{1/2}$) of all reactions were then determined by the equation *in vitro* $t_{1/2}$= 0.693/k. Conversion to *in vitro* CL_{int} (μl/min/mg) was achieved using Eq. 1 (6).

$$CL_{int} = \frac{0.693}{in\ vitro\ t_{1/2}} \cdot \frac{volume\ of\ incubation(\mu l)}{amount\ of\ microsomal\ protein\ in\ incubation(mg)} \quad (1)$$

This CL_{int}, determined with either UGT or P450 cofactors ($CL_{int,UGT}$ and $CL_{int,CYP}$, respectively) was corrected for experimentally determined fu_{inc} to give an unbound value for CL_{int} ($CL_{int,u}$).

Fraction metabolised. fm_{UGT} and fm_{CYP} values were calculated from the $CL_{int,u}$ values obtained in the presence of individual UGT and P450 cofactors, respectively, using Eqs. 2 and 3, respectively.

$$fm_{UGT} = \frac{CL_{int,UGT}}{CL_{int,UGT} + CL_{int,CYP}} \quad (2)$$

$$fm_{CYP} = \frac{CL_{int,CYP}}{CL_{int,UGT} + CL_{int,CYP}} \quad (3)$$

The *in vivo* estimates were obtained from the amount of the glucuronide excreted in the urine; potential contribution of the glucuronide metabolites excreted in the bile/faeces was not accounted for due to limited availability of such data.

Comparison of Intestinal and Hepatic $CL_{int,UGT}$. In order to allow valid comparison between the organs, clearance data were expressed per gram of tissue. Intestinal $CL_{int,UGT}$ and $CL_{int,CYP}$ values were scaled using an intestinal microsomal recovery value calculated from CYP3A homogenate protein levels reported by Paine *et al.* (30) (see Table II and "RESULTS"). A weighted scaling factor was estimated from the different sections of intestine to obtain an intestinal microsomal recovery value of 20.6 mg/g intestine. In the case of hepatic data, a standard human microsomal recovery of 40 mg/g liver was used (31).

Prediction of In Vivo Glucuronidation Clearance From In Vitro Hepatic Data. In vitro $CL_{int,UGT}$ obtained in HLM was scaled using a microsomal recovery of 40 mg protein/g liver (31) and a liver weight of 21.4 g liver/kg (32) to give a predicted *in vivo* $CL_{int,UGT}$ in ml/min/kg. Observed *in vivo* CL_{int} was calculated from both intravenous and oral literature data. *In vivo* values for intravenous plasma clearance ($CL_{i.v.}$), the blood to plasma concentration ratio (R_B) and the fraction unbound in plasma (fu_p) were used with the well-stirred liver model and a value for hepatic blood flow (Q_H) of 20.7 ml/min/kg (Eq. 4). Hepatic blood clearance (CL_b) was calculated by correcting $CL_{i.v.}$ for the R_B (7,32).

$$\text{Observed } CL_{int} = \frac{CL_b}{\frac{fu_p}{R_B} \cdot \left(1 - \frac{CL_b}{Q_H}\right)} \quad (4)$$

In the case of buprenorphine and naloxone, intravenous plasma clearance exceeded Q_H and therefore a value for CL_b was set at 90% of Q_H (i.e., 18.63 ml/min/kg). For two of the nine compounds (raloxifene and troglitazone), intravenous observed clearance data were not available. In addition to intravenous data, observed CL_{int} was also calculated from oral plasma clearance ($CL_{p.o.}$) values (assuming complete absorption from the gastrointestinal tract and no contribution of intestinal metabolism), as shown in Eq. 5. No oral clearance data were available in the case of buprenorphine and naloxone.

$$\text{Observed } CL_{int} = \frac{CL_{p.o.}}{fu_p / R_B} \quad (5)$$

When a value for R_B was not available, a value of either 1 or 0.55 (1—haematocrit) was assumed for basic and acidic compounds, respectively. In all instances, the observed CL_{int} was corrected for the *in vitro* fm_{UGT} obtained in HLM in order to give an *in vivo* estimate for $CL_{int,UGT}$.

Table II. Gut Metabolism Scaling Factors for Duodenum, Jejunum and Ileum

	Duodenum	Jejunum	Ileum
Microsomal CYP3A (pmol/mg)	30.6	22.6	16.6
Mucosal CYP3A (pmol/g mucosa)	445	463	391
Intestinal scaling factor (mg protein/g mucosa)[a]	14.5	20.5	23.5
Overall mucosal distribution (%)[b]	14	54	32

Data from Paine *et al.* (30)

[a] Total intestinal scaling factor (mg protein/g mucosa)=20.6 (weighted according to mucosal distribution)

[b] Estimated based on weight of mucosa, mucosal microsomal protein and mucosal CYP3A4 in each of the intestinal sections

RESULTS

Glucuronidation and P450 CL_{int} values were obtained for nine substrates in pooled HLM and HIM using a substrate depletion approach. The CL_{int} values were corrected for nonspecific microsomal binding using experimentally determined fu_{inc} (Table III), ranging from 0.07 to 0.95 in the case of troglitazone and mycophenolic acid, respectively. $CL_{int,UGT}$ values (Table III) ranged over four orders of magnitude in both the liver and intestine. Hepatic values were between 17–2,484 μl/min/mg for naloxone and quercetin, respectively, whereas intestinal $CL_{int,UGT}$ ranged from 18–4,259 μl/min/mg for mycophenolic acid and raloxifene, respectively. $CL_{int,CYP}$ values ranged from zero detection for mycophenolic acid and quercetin, up to 634 and 403 μl/min/mg for buprenorphine in HLM and HIM, respectively.

Substrate Depletion Profiles. Fig. 1 shows depletion profiles for all nine compounds in hepatic and intestinal microsomes at protein concentration of 0.1–1 mg/ml. For seven of the drugs investigated (diclofenac, gemfibrozil, mycophenolic acid, naloxone, quercetin, raloxifene and salbutamol), a higher clearance was seen by glucuronidation than by P450 metabolism in both HLM and HIM (Table III). The opposite was observed for buprenorphine in both organs and for the hepatic metabolism of troglitazone. Raloxifene and troglitazone showed a significantly higher clearance by glucuronidation in the intestine than in the liver (Table III), whereas this was comparable between the two organs for naloxone. Linear profiles (Fig. 1) were observed for all P450 reactions and for both the intestinal and hepatic glucuronidation of five drugs (buprenorphine, gemfibrozil, mycophenolic acid, salbutamol and raloxifene). However, in certain incubations, glucuronidation of the remaining four drugs followed a biphasic profile; in the intestine for naloxone and troglitazone, in the liver for quercetin and in both the intestine and liver for diclofenac. Where a biphasic depletion profile was observed, the initial linear phase was used to calculate CL_{int}.

Comparison of Intestinal and Hepatic $CL_{int,,UGT}$. Intestinal and hepatic clearance values were compared after scaling the microsomal data expressed per mg protein to per gram of organ, to give an indication of the relative importance of intestinal and hepatic glucuronidation and P450 metabolism. To achieve this, a scaling factor for human intestine was required. Paine *et al.* (30) reported CYP3A protein abundance in microsomal and mucosal samples from the duodenum, jejunum and ileum, prepared by mucosal scraping and analysed by Western blotting (Table II). A mean intestinal scaling factor of 20.6 mg microsomal protein per gram of mucosal tissue was calculated by weighting the regional factors according to mucosal distribution in the different sections of the intestine. Fig. 2A, B show a comparison of intestinal and hepatic $CL_{int,UGT}$ and $CL_{int,CYP}$ (per gram of organ), respectively, for the nine compounds investigated. As shown in Fig. 2A, $CL_{int,UGT}$ values were not correlated between the two organs ($r^2=0.04$). Two out of the nine drugs showed a higher $CL_{int,UGT}$ in the intestine than in the liver, giving a six- and nine-fold difference in the case of raloxifene and troglitazone, respectively. Naloxone showed an approximately equal $CL_{int,UGT}$ in both organs. In contrast, six drugs (buprenorphine, diclofenac, gemfibrozil, mycophenolic acid, quercetin and salbutamol) showed a higher glucuronidation clearance in the liver than in the intestine, ranging from a three- to 12-fold higher hepatic $CL_{int,UGT}$ for buprenorphine and gemfibrozil, respectively (five-fold on average).

Seven out of the nine drugs investigated (buprenorphine, diclofenac, gemfibrozil, naloxone, raloxifene, salbutamol and troglitazone) showed P450 clearance in addition to glucuronidation, as shown in Fig. 2B. Intestinal and hepatic $CL_{int,CYP}$ values were strongly correlated ($r^2=0.96$). For all drugs, $CL_{int,CYP}$ was higher in the liver than the intestine, ranging

Table III. Substrate Specificity for Different P450 and UGT Enzymes, Intestinal and Hepatic UGT and P450 Clearance in Liver and Intestinal Microsomes and Estimated *In Vitro* Extent of Glucuronidation for the Nine Compounds Investigated

			$CL_{int,u}$ (μl/min/mg)[c]					*In vitro* fm_{UGT}[d]	
			UGT		P450				
Compound	Major P450 specificity	Major UGT specificity[b]	HLM	HIM	HLM	HIM	fu_{inc} (1 mg/ml HLM)	HLM	HIM
Buprenorphine	CYP3A4	UGT1A1, UGT2B7	268	209	634	403	0.10	0.30	0.34
Diclofenac	CYP2C9	UGT1A9, UGT2B7	493	116	134	6.2	0.84	0.77	0.95
Gemfibrozil	CYP3A4	UGT2B7	114	19.2	26.7	1.1	0.91	0.81	0.95
Mycophenolic acid	–	UGT1A8	31.2	17.6	–	–	0.95	1.00	1.00
Naloxone	CYP3A4	UGT1A8, UGT2B7	17.4	21.4	14.5	7.7	0.87	0.55	0.73
Quercetin	–	UGT1A1, UGT1A8, UGT1A10	2,484	1,088	–	–	0.90	1.00	1.00
Raloxifene	CYP3A4	UGT1A1, UGT1A8, UGT1A10	376	4,259	164	97	0.08	0.74	0.97
Salbutamol	–[a]	–	19.9	10.0	10.9	8.0	0.88	0.65	0.56
Troglitazone	CYP3A4, CYP2C8	UGT1A1, UGT1A10	21.1	357	255	125	0.07	0.08	0.74

[a] Substantial sulphation
[b] From Kiang *et al.* (44), except quercetin (45)
[c] Data represent a mean from duplicate incubations in HLM pool A after correction for fu_{inc}
[d] The *in vitro* fm_{UGT} was estimated from clearances obtained in the presence of individual P450 or UGT cofactors (Eq. 2)

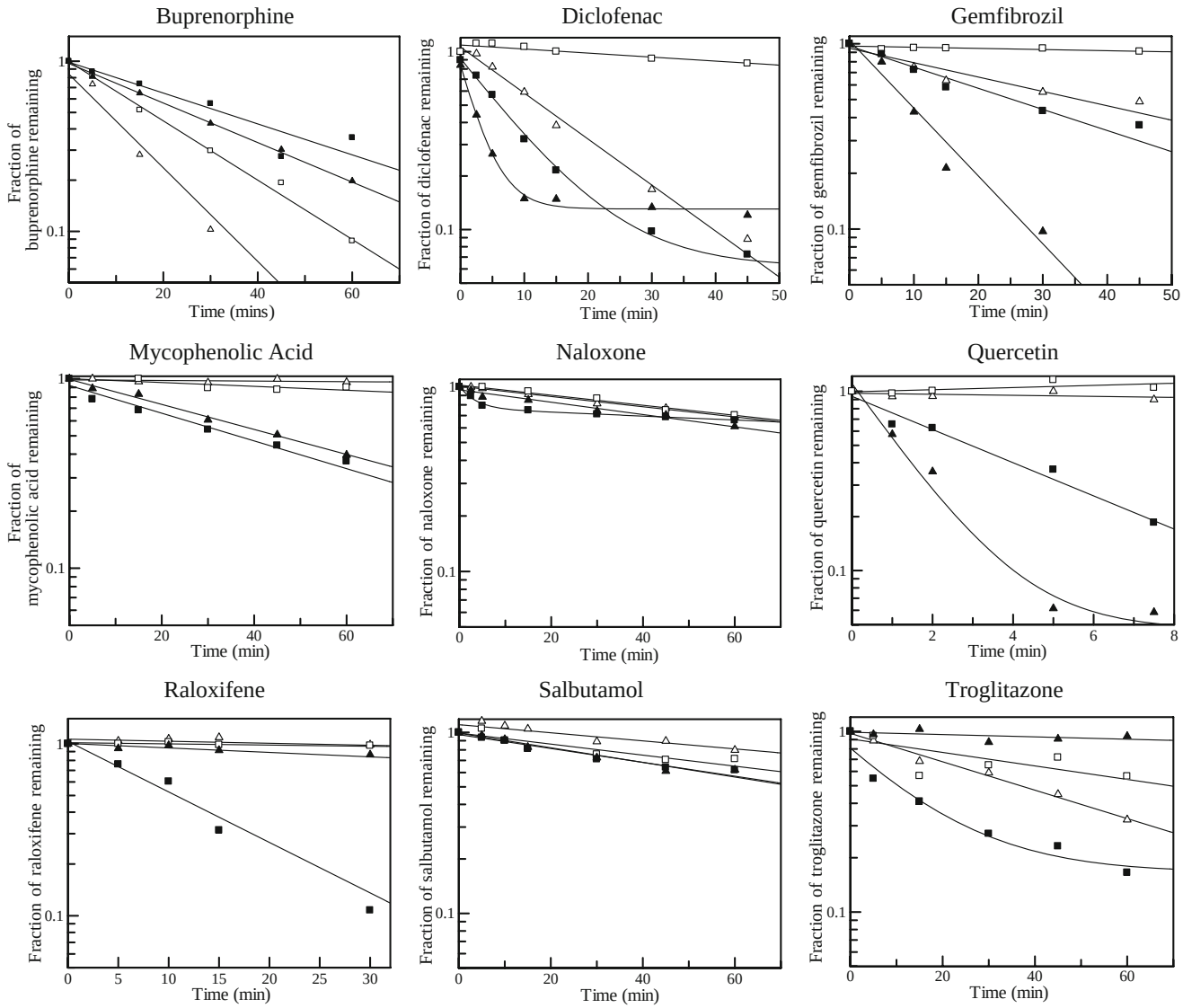

Fig. 1. Comparison of UGT and P450 depletion profiles in HLM and HIM. The hepatic *in vitro* data were obtained in HLM pool A. *Closed square* represents intestinal glucuronidation, *closed triangle* hepatic glucuronidation, *open square* intestinal P450 metabolism and *open triangle* hepatic P450 metabolism.

from a three-fold to a 47-fold difference for salbutamol and gemfibrozil, respectively. Raloxifene and troglitazone were compounds with a higher glucuronidation clearance in the intestine than the liver (Fig. 2A), but an intestinal P450 clearance was lower than hepatic (Fig. 2B). Excluding these two drugs, the trend for hepatic glucuronidation clearance was similar to that seen for P450 clearance.

$CL_{int,CYP}$ values for six compounds (buprenorphine, diclofenac, gemfibrozil, naloxone, raloxifene and troglitazone), selected by P450 enzyme specificity (Table III), were also corrected for the relative abundance of CYP3A4 and CYP2C9 in the liver (33) and intestine (17), as reported previously (18). Comparison of $CL_{int,CYP}$ normalized for CYP3A4 abundance in the corresponding organs (expressed as µl/min/pmolCYP) resulted in a two-fold higher $CL_{int,CYP3A4}$ in the intestine in comparison to the liver for buprenorphine, naloxone, raloxifene and troglitazone. The exception was gemfibrozil, where a seven-fold higher hepatic $CL_{int,CYP3A4}$ was seen. This contrasted with the initial findings (Table III) where hepatic $CL_{int,CYP}$ (expressed per g organ) was much higher for all drugs (15-fold on average). In both organs, the lowest and highest $CL_{int,CYP3A4}$ seen was for gemfibrozil and buprenorphine, ranging from 0.2 to 4.1 µl/min/$pmol_{CYP3A4}$ in the liver and from 0.03 to 9.4 µl/min/$pmol_{CYP3A4}$ in the intestine. In the case of diclofenac, hepatic $CL_{int,CYP2C9}$ was 2.5-fold higher than in the intestine (1.8 and 0.7 µl/min/$pmol_{CYP2C9}$ in the liver and intestine, respectively), in contrast to an initial 42-fold difference.

Fraction Metabolised by UGT and P450. Intestinal and hepatic fm_{UGT} and fm_{CYP} estimates were calculated from the $CL_{int,u}$ values obtained in the presence of individual UGT and P450 cofactors (Eqs. 2 and 3, respectively). The extent of glucuronidation ranged from 0.3 for buprenorphine to complete glucuronidation for mycophenolic acid and quercetin, as shown in Table III. A comparison of estimated fm_{UGT} values for the nine compounds investigated is illustrated in

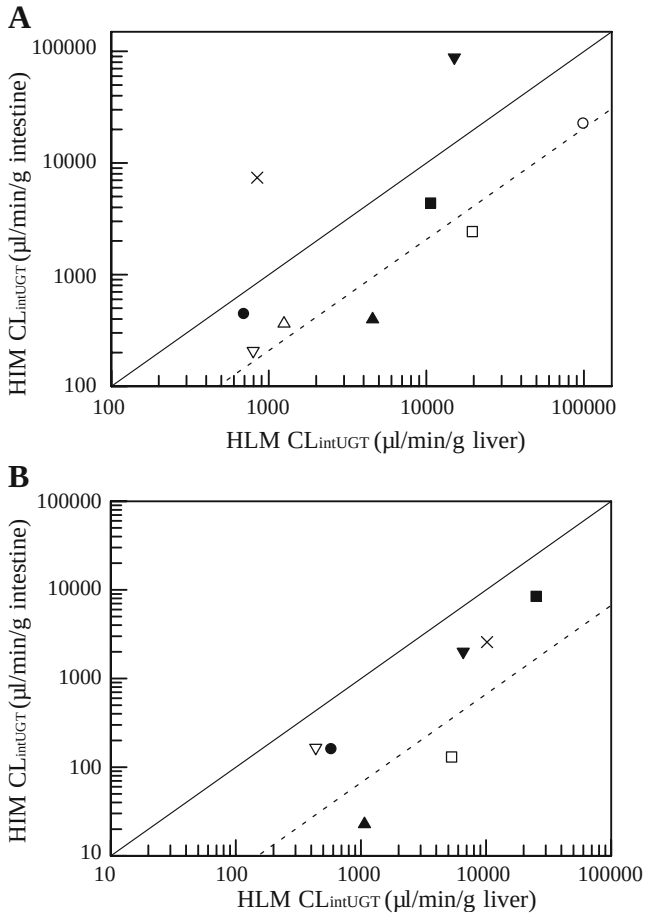

Fig. 2. Comparison of CL_{int} (expressed per g organ) in intestine and liver. The *solid lines* represent an equal clearance in HIM and HLM. The hepatic *in vitro* data were obtained in HLM pool A. **A** A comparison of $CL_{int,UGT}$ in the intestine and liver for nine compounds. The *dotted line* represents a five-fold higher hepatic than intestinal $CL_{int,UGT}$ (average difference seen excluding raloxifene and troglitazone). *Closed square* represents buprenorphine, *open square* diclofenac, *closed triangle* gemfibrozil, *open triangle* mycophenolic acid, *closed circle* naloxone, *open circle* quercetin, closed *inverted triangle* raloxifene, *open inverted triangle* salbutamol, *multiplication symbol* troglitazone. **B** A comparison of $CL_{int,CYP}$ in the intestine and liver for the seven compounds that showed P450 metabolism. The *dotted line* represents a 15-fold higher hepatic than intestinal $CL_{int,UGT}$ (average difference seen for all compounds): *closed square* represents buprenorphine, *open square* diclofenac, *closed triangle* gemfibrozil, *closed circle* naloxone, *closed inverted triangle* raloxifene, *open inverted triangle* salbutamol, *multiplication symbol* troglitazone.

Fig. 3. For most of the drugs in the dataset, the estimated extent of glucuronidation was in good agreement between HLM and HIM (r^2=0.76); with the exception of troglitazone, where a nine-fold difference was observed (74% and 8% in HIM and HLM, respectively). For six of the compounds, fm_{UGT} values were also estimated from *in vivo* renal excretion data, as described previously for fm_{CYP} (34). *In vivo* estimates of the extent of glucuronidation were comparable to *in vitro* values for buprenorphine, mycophenolic acid, naloxone, quercetin and raloxifene (Tables III and IV). However, for gemfibrozil, the estimated extent of glucuronidation *in vitro* exceeded the *in vivo* value (Table IV).

Prediction of In Vivo Clearance From In Vitro Hepatic Data. Scaled *in vitro* hepatic $CL_{int,UGT}$ was compared with human observed *in vivo* $CL_{int,UGT}$ from both intravenous and oral plasma clearances. The *in vivo* CL_{int}, R_B and fu_p values for all the drugs in the dataset are shown in Table IV. Fig. 4 shows the comparison of the predicted and observed $CL_{int,UGT}$ for the nine compounds investigated. Salbutamol and quercetin were the compounds with the lowest and highest values for *in vivo* observed $CL_{int,UGT}$, respectively, ranging from 3–2,608 ml/min/kg for estimates obtained from intravenous clearance and 16–930,000 ml/min/kg from the oral data. On average, predicted $CL_{int,UGT}$ was 22% of the observed intravenous CL_{int} value for the seven compounds where these *in vivo* data were available (Fig. 4A). Gemfibrozil and salbutamol were over-predicted, by two- and nine-fold, respectively, whereas for the other five compounds prediction represented 6–82% of the *in vivo* value (for naloxone and quercetin, respectively). In contrast, predicted $CL_{int,UGT}$ was on average only 1.4% of the observed oral CL_{int} data (Fig. 4B). For four of the compounds (diclofenac, gemfibrozil, mycophenolic acid and salbutamol), the $CL_{int,UGT}$ from oral clearance data was predicted well (on average 93% of *in vivo* value), whereas the prediction was only 0.2% of the observed value for quercetin and 3% for raloxifene and troglitazone. In the case of drugs where under-prediction was observed, the difference between the observed oral and predicted $CL_{int,UGT}$ correlated well with the intestinal $CL_{int,UGT}$ (expressed per g organ), supporting the importance of intestinal contribution (Fig. 4C).

Importance of the Choice of Pooled Liver Microsomes. The impact of different liver sources on hepatic $CL_{int,UGT}$ was assessed for the pronounced outliers, raloxifene and troglitazone (Table V). $CL_{int,UGT}$ values obtained from three different pools of HLM (A–C) ranged between 30–394 µl/min/mg for raloxifene and 21–166 µl/min/mg for troglitazone, as shown in Table V. In comparison, $CL_{int,CYP}$ varied between

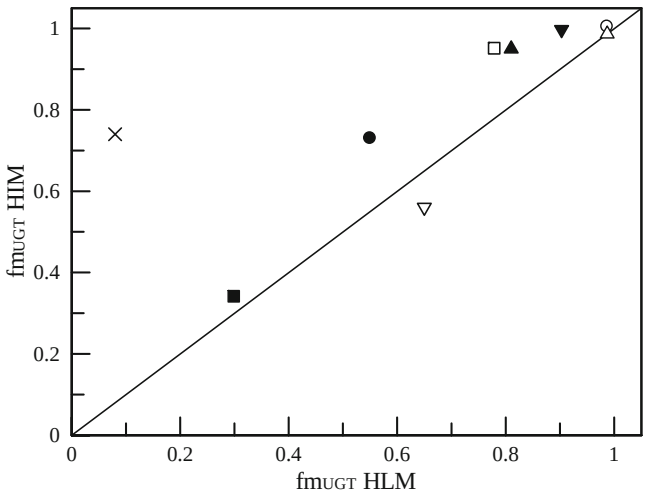

Fig. 3. Comparison of *in vitro* fm_{UGT} in the liver and intestine for nine substrates. The *line* represents an equal fm_{UGT} in HLM and HIM. The hepatic *in vitro* data were obtained in HLM pool A. *Closed square* represents buprenorphine, *open square* diclofenac, *closed triangle* gemfibrozil, *open triangle* mycophenolic acid, *closed circle* naloxone, *open circle* quercetin, *closed inverted triangle* raloxifene, *open inverted triangle* salbutamol, *multiplication symbol* troglitazone.

Table IV. Published Intravenous and Oral *In Vivo* Values for CL_{int} and R_B, fu_p and fm_{UGT} Values

Compound		Observed *in vivo* plasma clearance (ml/min/kg)			Observed *in vivo* CL_{int} (ml/min/kg)		Observed *in vivo* CL_{int} corrected for fm_{UGT} (ml/min/kg)		R_B	fu_p		*In vivo* fm_{UGT}[d]	
		i.v.		p.o.	i.v.	p.o.	i.v.	p.o.					
Buprenorphine	Base	19	(46)	–	2,795[a]	–	838	–	0.6	(9)	0.04	(46)	0.5	(47)
Diclofenac	Acid	3.5	(46)	8	(48)	1,011	881	778	678	0.55	(7)	0.005	(46)	–	–
Gemfibrozil	Acid	1.7	(49)	1.7	(50)	66	32	54	26	0.55	(7)	0.03	(7)	0.4	(47)
Mycophenolic acid	Acid	3.3	(51)	3.5	(51)	186	77	186	77	0.55[b]	Estimated	0.025	(49)	0.9	(52)
Naloxone	Base	23	(46)	–		477[a]	–	262	–	1.22	(7)	0.54	(46)	0.65	(10)
Quercetin	Base	11	(46)	8,333	(53)	2,608	930,000	2,608	930,000	1[c]	Estimated	0.009	(46)	0.99[e]	–
Raloxifene	Base	–		735	(54)	–	15,000	–	11,000	1[c]	Estimated	0.05	(54)	0.9	(16)
Salbutamol	Base	2.4	(55)	15	(56)	2.9	16	1.9	10	1[c]	Estimated	0.925	(57)	–	–
Troglitazone	Neutral	–		13.1	(58)	–	7,629	–	610	0.55	(58)	0.0009	(58)	–	–

[a] CL_b assumed to be 90% of Q_H (18.63 ml/min/kg) because actual $CL_b > Q_H$
[b] Assumed to be 0.55 for acidic drugs
[c] Assumed to be 1 for basic drugs
[d] *In vivo* fm_{UGT} values from renal excretion data
[e] Includes also contribution of sulphate conjugates. Dashes represent unavailable clearance or *in vivo* fm_{UGT} data

133–198 μl/min/mg for raloxifene and 34–255 μl/min/mg for troglitazone. For raloxifene, the ratio of hepatic to intestinal $CL_{int,UGT}$ was comparable between lots A and B, whereas in the case of C, the hepatic $CL_{int,UGT}$ was significantly lower, giving a more than ten-fold difference from the other two lots. In contrast, troglitazone showed a similar hepatic to intestinal $CL_{int,UGT}$ ratio using pools B and C, compared with the initial nine-fold higher intestinal $CL_{int,UGT}$ seen using pool A; this trend was also apparent in the case of P450 metabolism. The fold difference between the intestinal and hepatic $CL_{int,CYP}$ of raloxifene was comparable in all three lots of HLM analysed. The *in vitro* hepatic fm_{UGT} estimated for raloxifene was comparable between HLM lots A and B (74% and 67%, respectively), but lower using lot C (18%). For troglitazone, hepatic fm_{UGT} estimates using B (83%) and C (58%) were significantly higher than in A (8%) and, as such, were comparable to the intestinal value (74%). However, the overall prediction success of the *in vivo* glucuronidation clearance for raloxifene and troglitazone (3%) did not change significantly between the three HLM pools.

DISCUSSION

An increasing awareness of the importance of conjugation metabolism has led to a need for the incorporation of these pathways into drug clearance prediction. At present, limited published data are available on the contribution of intestinal glucuronidation to overall clearance, which could be a potential contributor to the under-prediction of *in vivo* clearance based solely on *in vitro* hepatic data (1,9–11). In addition, there is inconsistency in available data, and this can be rationalised by differences in the enterocyte isolation method, segment of the intestine used (proximal or the whole length), source of the intestinal tissue (individual or pooled) and UGT activation method (10,24,26). Therefore, the aim of the current study was to perform a comprehensive analysis of the relative importance of intestinal glucuronidation in comparison to the liver for a range of compounds using standardised *in vitro* conditions.

A number of studies have reported higher $CL_{int,UGT}$ values when the pore forming agent alamethicin was used to activate the microsomes (25–27) in comparison to the detergent (23), sonication (35) or no activation method (22). This is consistent with other publications where the usefulness of alamethicin as an activating agent has been reported (13,14) and hence was used in this study. Recent studies have reported that the presence of 2% bovine serum albumin in the microsomal incubation increases the clearance estimates for UGT2B7 and UGT1A9 substrates (36–38). However, the effect on a number of intestine specific UGTs is still unknown.

Current study has shown that seven of the nine drugs investigated had a higher clearance by glucuronidation than by P450 metabolism in both the liver and intestine. Buprenorphine was the only compound where the opposite trend was observed in both organs. This was consistent with renal excretion data reported, as shown in Table IV. For raloxifene and troglitazone, a higher clearance by glucuronidation than by P450 metabolism was seen in the intestine. The *in vitro* extent of glucuronidation obtained in the present study was

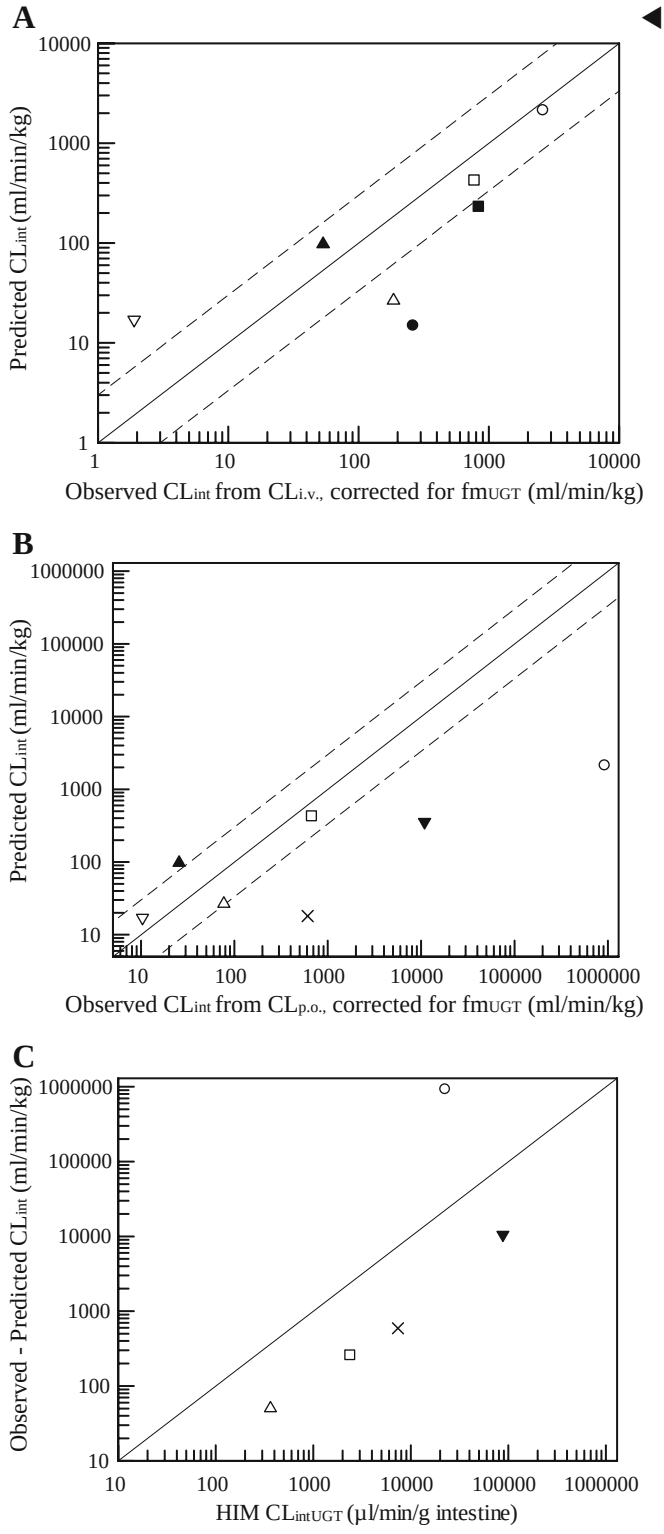

Fig. 4. Prediction of *in vivo* intrinsic clearance from *in vitro* hepatic glucuronidation data for nine compounds. $CL_{int,UGT}$ (obtained in HLM pool A) was scaled using a microsomal recovery of 40 mg protein/g liver (31), a liver weight of 21.4 g liver/kg and modelled with the well-stirred liver model (32). *In vivo* $CL_{int,u}$ was calculated from literature values of plasma clearance, R_B and fu_p (Table IV) and corrected for fm_{UGT} obtained in HLM (Table III) in order to give *in vivo* values for glucuronidation clearance. The *solid lines* represent an equal observed and predicted clearance and the *dotted lines* represent a three-fold difference from the line of unity. *Closed square* represents buprenorphine, *open square* diclofenac, *closed triangle* gemfibrozil, *open triangle* mycophenolic acid, *closed circle* naloxone, *open circle* quercetin, *closed inverted triangle* raloxifene, *open inverted triangle* salbutamol and *multiplication symbol* troglitazone. Observed $CL_{int,UGT}$ obtained from intravenous data (**A**) and oral clearance data (**B**). **C** Comparison of the difference between observed oral and predicted $CL_{int,UGT}$ and intestinal $CL_{int,UGT}$ (expressed per g organ) for drugs showing clearance under-prediction. *Open square* represents diclofenac, *open triangle* mycophenolic acid, *open circle* quercetin, *closed inverted triangle* raloxifene, and *multiplication symbol* troglitazone.

comparable to published *in vivo* fm_{UGT} values for five of the drugs studied, showing an ability to accurately estimate fm_{UGT} from *in vitro* data using microsomes and different cofactor conditions. The extent of glucuronidation for gemfibrozil, however, was higher *in vitro* than that found *in vivo*. Gemfibrozil forms acyl glucuronides (39), which are unstable in biological samples at physiological pH (40), which could lead to the underestimation of the extent of glucuronidation *in vivo*. The ability to determine fm_{UGT} from *in vitro* data could have implications in the prediction of UGT-mediated clinical drug–drug interactions, analogous to the approach recently reported for fm_{CYP} estimates (41). However, cautious interpretation of this *in vitro* approach is required due to the lack of information on the potential contribution of renal clearance to drug elimination (as for the remaining three drugs in this study).

As shown in Fig. 1, biexponential depletion profiles were observed for both intestinal and hepatic glucuronidation, in five of the 36 curves generated. These biphasic profiles have been previously rationalised by a decreased enzyme activity in microsomes over time, enhanced by poor mixing and reduced oxygen availability at higher protein concentrations (42). However, in this study, the second phase in these profiles occurred too rapidly for this to be an explanation, especially for quercetin; depletion was complete within 5 min. Also, the protein concentration used for both quercetin and raloxifene was very low (0.1 mg/ml). Another explanation for the biphasic profiles could be end-product inhibition, where the increasing concentration of metabolites may interact with the enzyme and stop further metabolism of the parent compound (42).

To our knowledge, intestinal human scaling factors have not been reported, hence there is no analogous agreement to that reached for the scaling of hepatic data (31). In the current study, $CL_{int,UGT}$ were scaled per gram of organ using an intestinal microsomal recovery value of 20.6 mg protein/g intestine, calculated from data by Paine *et al.* (30). This is lower than a standard value for human liver of 40 mg protein/g liver (31). These scaling factors would have no effect on the estimation of the fm_{UGT} in the liver and intestine in this study, but they would have an impact on the assessment of the importance of intestinal glucuronidation relative to the liver. The relative assessment of hepatic and intestinal glucuronidation was also dependent on the pool of microsomes used, as illustrated in the example of raloxifene and troglitazone (Table V). The importance of intestinal glucuronidation for raloxifene was consistent across additional pools of HLM; however, for troglitazone, hepatic $CL_{int,UGT}$ (B and C)

Table V. *In Vitro* $CL_{int,UGT}$ and $CL_{int,CYP}$ from Three Different Pools of HLM and Comparison with Intestinal Values

Compound	HLM pool	*In vitro* hepatic $CL_{int,UGT}$ (μl/min/mg)	Hepatic:intestinal $CL_{int,UGT}$ ratio[a]	*In vitro* hepatic $CL_{int,CYP}$ (μl/min/mg)	Hepatic:intestinal $CL_{int,CYP}$ ratio[a]
Raloxifene	A (n=30)	376	1:6	164	3:1
	B (n=22)	394	1:6	198	4:1
	C (n=33)	30	1:73	133	3:1
Troglitazone	A (n=30)	21	1:9	255	4:1
	B (n=22)	166	1:1	34	1:2
	C (n=33)	148	1:1	108	2:1

[a] From intestinal and hepatic $CL_{int,UGT}$ values scaled per gram of organ using 20.6 mg protein/g intestine and 40 mg protein/g liver, respectively

became more comparable to the intestinal value seen. Differences in $CL_{int,UGT}$ and $CL_{int,CYP}$ did not appear to correlate with UGT1A1 or P450 activity data known for the three HLM pools and were not similar for the two drugs. However, enzyme activity was not known for other enzymes of interest, such as UGT2B7. The hepatic under-prediction of *in vivo* clearance, consistently occurred for both drugs regardless of the HLM pool used, and to a much larger degree than for the other compounds.

The significantly lower extent of glucuronidation in the liver in comparison to the intestine observed for these two compounds was not surprising, as recombinant UGT data have shown raloxifene and troglitazone to be substrates for the intestinal specific UGT1A8 and UGT1A10. Kemp *et al.* (25) have shown that raloxifene is conjugated to two UGT metabolites, the 4′-β- and 6-β-glucuronide, which are predominantly formed via UGT1A10 and UGT1A8, respectively. Raloxifene Km values for UGT1A8 and UGT1A10 are below 10 μM, indicating a high affinity for these intestinal UGTs. Troglitazone has shown comparable affinity for UGT1A10 (Km 11 μM), but recombinant data also indicate the contribution of UGT1A8, UGT1A1 and UGT2B7 (26). The relative abundance of the different UGTs is unknown and therefore, the explicit contribution of UGT1A8 and UGT1A10 to the overall clearance in comparison to UGTs present both in the liver and the intestine (UGT1A1 and UGT2B7), is difficult to assess. In contrast to troglitazone and raloxifene, gemfibrozil had a 12-fold higher hepatic than intestinal $CL_{int,UGT}$, when scaled per gram of organ. This is consistent with a recent study reporting negligible affinity of gemfibrozil for the intestinal specific UGTs and glucuronidation mainly by UGT2B7 (43).

For the seven compounds where P450 metabolism was observed, a higher $CL_{int,CYP}$ was seen in the liver than the intestine. An additional analysis was made of the data for the drugs buprenorphine, diclofenac, gemfibrozil, naloxone, raloxifene and troglitazone, since the abundance data for P450 enzymes contributing to their clearance (CYP3A4 and CYP2C9) were available (33). Correcting clearance for enzyme abundance and expressing it per pmol of relevant P450 enzyme, increased the apparent importance of intestinal metabolism significantly for all compounds. This confirms the importance of enzyme abundance data for *in vitro–in vivo* extrapolation (8,18) and highlights the need for corresponding data on UGTs.

In addition to an analysis of the importance of the intestine to the metabolism of the selected compounds, this study investigated the prediction of *in vivo* clearance from the *in vitro* hepatic data. On average, predicted $CL_{int,UGT}$ represents 22% of *in vivo* $CL_{int,UGT}$ obtained from intravenous clearance data for the drugs in this dataset. This under-prediction trend is consistent with previous reports of approximately ten-fold (1,10,11). Buprenorphine, diclofenac and gemfibrozil were predicted well from the *in vitro* hepatic data, and these drugs had no significant intestinal glucuronidation clearance when compared to the liver (Fig. 4). This suggests that alamethicin activated human liver microsomes can be used to successfully predict glucuronidation clearance for drugs with no significant contribution of intestinal glucuronidation. For four drugs (diclofenac, gemfibrozil, mycophenolic acid and salbutamol), prediction success was similar regardless of whether an intravenous or oral *in vivo* clearance was used. In contrast, the prediction of quercetin oral $CL_{int,UGT}$ was significantly lower (0.2%) than that of the intravenous clearance (82%). Oral predictions were also poor (3%) for raloxifene and troglitazone, which is not surprising considering that these predictions assume that the fraction of drug escaping intestinal extraction is 1. This is of limited use in the case of significant intestinal metabolism, as illustrated particularly for raloxifene and troglitazone (Table III). The difference between the observed oral and predicted $CL_{int,UGT}$ for these drugs correlated well with the intestinal $CL_{int,UGT}$ (expressed per g organ), highlighting the importance of intestinal contribution (Fig. 4C). The potential contribution of other conjugation enzymes (e.g., sulphotransferases) to the hepatic and intestinal clearance of some of the drugs investigated (e.g., salbutamol, troglitazone), as well as extra-hepatic metabolism in other organs to the intestine, represent additional confounding factors.

In conclusion, current study has shown that alamethicin activated microsomes provide a valuable method of analysis of the importance of intestinal glucuronidation in comparison to that in the liver. The use of the corresponding P450 and UGT cofactors allows assessment of the fraction glucuronidated *in vitro* in both organs. There is much circumstantial evidence suggesting that the intestinal glucuronidation will affect the *in vivo* clearance of some drugs and, as such, the prediction of clearance when based solely on hepatic data. Incorporation of intestinal glucuronidation into clearance prediction using appropriate combined liver and intestinal physiologically-based pharmacokinetic model is required, in particular for compounds with a significant contribution of intestine specific UGTs (UGT1A8, 1A10) to their clearance.

ACKNOWLEDGEMENTS

The Authors would like to thank Sue Murby and Dr David Hallifax (University of Manchester) for valuable assistance with the LC-MS/MS.

The work was funded by a consortium of pharmaceutical companies (GlaxoSmithKline, Lilly, Novartis, Pfizer and Servier) within the Centre for Applied Pharmacokinetic Research at the University of Manchester. Part of this study was presented at the 10th ISSX Meeting, May 18–21, 2008, Vienna, Austria.

REFERENCES

1. J. O. Miners *et al*. *In vitro–in vivo* correlation for drugs and other compounds eliminated by glucuronidation in humans: pitfalls and promises. *Biochem. Pharmacol.* **71**(11):1531–1539 (2006). doi:10.1016/j.bcp.2005.12.019.
2. J. A. Williams *et al*. Drug–drug interactions for UDP-glucuronosyltransferase substrates: a pharmacokinetic explanation for typically observed low exposure (AUCi/AUC) ratios. *Drug Metab. Dispos.* **32**(11):1201–1208 (2004). doi:10.1124/dmd.104.000794.
3. J. B. Houston. Utility of *in vitro* drug metabolism data in predicting *in vivo* metabolic clearance. *Biochem. Pharmacol.* **47**(9):1469–1479 (1994). doi:10.1016/0006-2952(94)90520-7.
4. R. J. Riley, D. F. McGinnity, and R. P. Austin. A unified model for predicting human hepatic, metabolic clearance from *in vitro* intrinsic clearance data in hepatocytes and microsomes. *Drug Metab. Dispos.* **33**(9):1304–1311 (2005). doi:10.1124/dmd.105.004259.
5. H. C. Rawden *et al.* Microsomal prediction of *in vivo* clearance and associated interindividual variability of six benzodiazepines in humans. *Xenobiotica.* **35**(6):603–625 (2005). doi:10.1080/00498250500162870.
6. R. S. Obach. Prediction of human clearance of twenty-nine drugs from hepatic microsomal intrinsic clearance data: An examination of *in vitro* half-life approach and nonspecific binding to microsomes. *Drug Metab. Dispos.* **27**(11):1350–1359 (1999).
7. H. S. Brown, M. Griffin, and J. B. Houston. Evaluation of cryopreserved human hepatocytes as an alternative *in vitro* system to microsomes for the prediction of metabolic clearance. *Drug Metab. Dispos.* **35**(2):293–301 (2007). doi:10.1124/dmd.106.011569.
8. A. Rostami-Hodjegan, and G. T. Tucker. Simulation and prediction of *in vivo* drug metabolism in human populations from *in vitro* data. *Nat. Rev. Drug Discov.* **6**(2):140–148 (2007). doi:10.1038/nrd2173.
9. M. Mistry, and J. B. Houston. Glucuronidation *in vitro* and *in vivo*. Comparison of intestinal and hepatic conjugation of morphine, naloxone, and buprenorphine. *Drug Metab. Dispos.* **15**(5):710–717 (1987).
10. M. G. Soars, B. Burchell, and R. J. Riley. *In vitro* analysis of human drug glucuronidation and prediction of *in vivo* metabolic clearance. *J. Pharmacol. Exp. Ther.* **301**(1):382–390 (2002). doi:10.1124/jpet.301.1.382.
11. S. Boase, and J. O. Miners. *In vitro–in vivo* correlations for drugs eliminated by glucuronidation: investigations with the model substrate zidovudine. *Br. J. Clin. Pharmacol.* **54**(5):493–503 (2002). doi:10.1046/j.1365-2125.2002.01669.x.
12. J. J. Engtrakul *et al.* Altered AZT (3′-azido-3′-deoxythymidine) glucuronidation kinetics in liver microsomes as an explanation for underprediction of *in vivo* clearance: comparison to hepatocytes and effect of incubation environment. *Drug Metab. Dispos.* **33**(11):1621–1627 (2005). doi:10.1124/dmd.105.005058.
13. M. B. Fisher *et al*. *In vitro* glucuronidation using human liver microsomes and the pore-forming peptide alamethicin. *Drug Metab. Dispos.* **28**(5):560–566 (2000).
14. M. G. Soars, B. J. Ring, and S. A. Wrighton. The effect of incubation conditions on the enzyme kinetics of udp-glucuronosyltransferases. *Drug Metab. Dispos.* **31**(6):762–767 (2003). doi:10.1124/dmd.31.6.762.
15. M. B. Fisher *et al*. The role of hepatic and extrahepatic UDP-glucuronosyltransferases in human drug metabolism. *Drug Metab. Rev.* **33**(3–4):273–297 (2001). doi:10.1081/DMR-120000653.
16. J. K. Ritter. Intestinal UGTs as potential modifiers of pharmacokinetics and biological responses to drugs and xenobiotics. *Expert. Opin. Drug Metab. Toxicol.* **3**(1):93–107 (2007). doi:10.1517/17425255.3.1.93.
17. M. F. Paine *et al.* The human intestinal cytochrome P450 “pie”. *Drug Metab. Dispos.* **34**(5):880–886 (2006). doi:10.1124/dmd.105.008672.
18. A. Galetin, and J. B. Houston. Intestinal and hepatic metabolic activity of five cytochrome P450 enzymes—impact on prediction of first-pass metabolism. *J. Pharmacol. Exp. Ther.* **318**(3):1220–1229 (2006). doi:10.1124/jpet.106.106013.
19. R. H. Tukey, and C. P. Strassburg. Genetic multiplicity of the human UDP-glucuronosyltransferases and regulation in the gastrointestinal tract. *Mol. Pharmacol.* **59**(3):405–414 (2001).
20. J. H. Lin, M. Chiba, and T. A. Baillie. Is the role of the small intestine in first-pass metabolism overemphasized? *Pharmacol. Rev.* **51**(2):135–158 (1999).
21. X. Cao *et al.* Why is it challenging to predict intestinal drug absorption and oral bioavailability in human using rat model. *Pharm. Res.* **23**(8):1675–1686 (2006). doi:10.1007/s11095-006-9041-2.
22. O. Bernard, and C. Guillemette. The main role of UGT1A9 in the hepatic metabolism of mycophenolic acid and the effects of naturally occurring variants. *Drug Metab. Dispos.* **32**(8):775–778 (2004). doi:10.1124/dmd.32.8.775.
23. K. Bowalgaha, and J. O. Miners. The glucuronidation of mycophenolic acid by human liver, kidney and jejunum microsomes. *Br. J. Clin. Pharmacol.* **52**(5):605–609 (2001). doi:10.1046/j.0306-5251.2001.01487.x.
24. E. J. Jeong *et al.* Species- and disposition model-dependent metabolism of raloxifene in gut and liver: role of UGT1A10. *Drug Metab. Dispos.* **33**(6):785–794 (2005). doi:10.1124/dmd.104.001883.
25. D. C. Kemp, P. W. Fan, and J. C. Stevens. Characterization of raloxifene glucuronidation *in vitro*: contribution of intestinal metabolism to presystemic clearance. *Drug Metab. Dispos.* **30**(6):694–700 (2002). doi:10.1124/dmd.30.6.694.
26. Y. Watanabe, M. Nakajima, and T. Yokoi. Troglitazone glucuronidation in human liver and intestine microsomes: high catalytic activity of UGT1A8 and UGT1A10. *Drug Metab. Dispos.* **30**(12):1462–1469 (2002). doi:10.1124/dmd.30.12.1462.
27. E. J. Jeong, H. Lin, and M. Hu. Disposition mechanisms of raloxifene in the human intestinal Caco-2 model. *J. Pharmacol. Exp. Ther.* **310**(1):376–385 (2004). doi:10.1124/jpet.103.063925.
28. M. Gertz *et al.* Drug lipophilicity and microsomal protein concentration as determinants in the prediction of the fraction unbound in microsomal incubations. *Drug Metab. Dispos.* **36**(3):535–542 (2008). doi:10.1124/dmd.107.018713.
29. D. Hallifax, and J. B. Houston. Binding of drugs to hepatic microsomes: comment and assessment of current prediction methodology with recommendation for improvement. *Drug Metab. Dispos.* **34**(4):724–726 (2006). author reply 727, doi:10.1124/dmd.105.007658.
30. M. F. Paine *et al*. Characterization of interintestinal and intraintestinal variations in human CYP3A-dependent metabolism. *J. Pharmacol. Exp. Ther.* **283**(3):1552–1562 (1997).
31. Z. E. Barter *et al*. Scaling factors for the extrapolation of *in vivo* metabolic drug clearance from *in vitro* data: reaching a consensus on values of human microsomal protein and hepatocellularity per gram of liver. *Curr. Drug Metab.* **8**(1):33–45 (2007). doi:10.2174/138920007779315053.
32. K. Ito, and J. B. Houston. Prediction of human drug clearance from *in vitro* and preclinical data using physiologically based and empirical approaches. *Pharm. Res.* **22**(1):103–112 (2005). doi:10.1007/s11095-004-9015-1.
33. K. R. Yeo, A. Rostami-Hodjegan, and G. T. Tucker. Abundance of cytochrome P450 in human liver: a meta-analysis. *Br. J. Clin. Pharmacol.* **57**:687–688 (2004).
34. H. S. Brown et al. Prediction of *in vivo* drug–drug interactions from *in vitro* data: impact of incorporating parallel pathways of drug elimination and inhibitor absorption rate constant. *Br. J. Clin. Pharmacol.* **60**(5):508–518 (2005). doi:10.1111/j.1365-2125.2005.02483.x.
35. A. G. Staines, M. W. Coughtrie, and B. Burchell. N-glucuronidation of carbamazepine in human tissues is mediated by

UGT2B7. *J. Pharmacol. Exp. Ther.* **311**(3):1131–1137 (2004). doi:10.1124/jpet.104.073114.
36. P. J. Kilford *et al*. Prediction of drug clearance by glucuronidation from *in vitro* data: Use of combined P450 and UGT cofactors in alamethicin activated human liver microsomes. *Drug Metab. Dispos.* **37**(1):82–89 (2009).
37. A. Rowland *et al*. Binding of inhibitory fatty acids is responsible for the enhancement of UDP-glucuronosyltransferase 2B7 activity by albumin: implications for *in vitro–in vivo* extrapolation. *J. Pharmacol. Exp. Ther.* **321**(1):137–147 (2007). doi:10.1124/jpet.106.118216.
38. A. Rowland *et al*. The "albumin effect" and drug glucuronidation: bovine serum albumin and fatty acid-free human serum albumin enhance the glucuronidation of UDP-glucuronosyltransferase (UGT) 1A9 substrates but not UGT1A1 and UGT1A6 activities. *Drug Metab. Dispos.* **36**(6):1056–1062 (2008). doi:10.1124/dmd.108.021105.
39. B. C. Sallustio, B. A. Fairchild, and P. R. Pannall. Interaction of human serum albumin with the electrophilic metabolite 1-O-gemfibrozil-beta-D-glucuronide. *Drug Metab. Dispos.* **25**(1):55–60 (1997).
40. H. Spahn-Langguth, and L. Z. Benet. Acyl glucuronides revisited: is the glucuronidation process a toxification as well as a detoxification mechanism? *Drug Metab. Rev.* **24**(1):5–47 (1992). doi:10.3109/03602539208996289.
41. K. A. Youdim. Application of CYP3A4 *in vitro* data to predict clinical drug–drug interactions; predictions of compounds as objects of interaction. *Br. J. Clin. Pharmacol.* **65**(5):680–692 (2008).
42. H. M. Jones, and J. B. Houston. Substrate depletion approach for determining *in vitro* metabolic clearance: time dependencies in hepatocyte and microsomal incubations. *Drug Metab. Dispos.* **32**(9):973–982 (2004). doi:10.1124/dmd.104.000125.
43. Y. Mano, T. Usui, and H. Kamimura. The UDP-glucuronosyltransferase 2B7 isozyme is responsible for gemfibrozil glucuronidation in the human liver. *Drug Metab. Dispos.* **35**(11):2040–2044 (2007). doi:10.1124/dmd.107.017269.
44. T. K. Kiang, M. H. Ensom, and T. K. Chang. UDP-glucuronosyltransferases and clinical drug–drug interactions. *Pharmacol. Ther.* **106**(1):97–132 (2005). doi:10.1016/j.pharmthera.2004.10.013.
45. Y. K. Chen *et al.* Quantitative regioselectivity of glucuronidation of quercetin by recombinant UDP-glucuronosyltransferases 1A9 and 1A3 using enzymatic kinetic parameters. *Xenobiotica.* **35**(10–11):943–954 (2005). doi:10.1080/00498250500372172.
46. R. S. Obach, F. Lombardo, and N. J. Waters. Trend analysis of a database of intravenous pharmacokinetic parameters in humans for 670 drug compounds. *Drug Metab. Dispos.* **36**(7):1385–1405 (2008).
47. R. J. Bertz, and G. R. Granneman. Use of *in vitro* and *in vivo* data to estimate the likelihood of metabolic pharmacokinetic interactions. *Clin. Pharmacokinet.* **32**(3):210–258 (1997).
48. J. V. Willis *et al.* The pharmacokinetics of diclofenac sodium following intravenous and oral administration. *Eur. J. Clin. Pharmacol.* **16**(6):405–410 (1979). doi:10.1007/BF00568201.
49. K. E. Thummel, D. D. Shen, N. Isoherranen, and H. E. Smith. Goodman & Gilman's the pharmacological basis of therapeutics. 11th Edition. In L.L. Brunton (ed.), *Section XV—Toxicology. Appendix II. Design and Optimization of Dosage Regimens: Pharmacokinetic Data. 11th ed*. McGraw-Hill Medical Division, New York, 2006.
50. M. B. Rouini, M. Baluchestani, and L. Hakemi. Study of dose-linearity of gemfibrozil pharmacokinetics in human. *Int. J. Pharmacol.* **2**(1):75–78 (2006).
51. R. Bullingham *et al.* Pharmacokinetics and bioavailability of mycophenolate mofetil in healthy subjects after single-dose oral and intravenous administration. *J. Clin. Pharmacol.* **36**(4):315–324 (1996).
52. K. K. Miles *et al.* An investigation of human and rat liver microsomal mycophenolic acid glucuronidation: evidence for a principal role of UGT1A enzymes and species differences in UGT1A specificity. *Drug Metab. Dispos.* **33**(10):1513–1520 (2005). doi:10.1124/dmd.105.004663.
53. Y. J. Moon *et al.* Quercetin pharmacokinetics in humans. *Biopharm. Drug Dispos.* **29**(4):205–217 (2008). doi:10.1002/bdd.605.
54. D. Hochner-Celnikier. Pharmacokinetics of raloxifene and its clinical application. *Eur. J. Obstet. Gynecol.* **85**:23–29 (1999). doi:10.1016/S0301-2115(98)00278-4.
55. E. Rey *et al.* Pharmacokinetics of intravenous salbutamol in renal insufficiency and its biological effects. *Eur. J. Clin. Pharmacol.* **37**(4):387–389 (1989). doi:10.1007/BF00558505.
56. D. A. Goldstein, Y. K. Tan, and S. J. Soldin. Pharmacokinetics and absolute bioavailability of salbutamol in healthy adult volunteers. *Eur. J. Clin. Pharmacol.* **32**(6):631–634 (1987). doi:10.1007/BF02456001.
57. D. J. Morgan *et al.* Pharmacokinetics of intravenous and oral salbutamol and its sulphate conjugate. *Br. J. Clin. Pharmacol.* **22**(5):587–593 (1986).
58. Y. Naritomi *et al.* Utility of hepatocytes in predicting drug metabolism: comparison of hepatic intrinsic clearance in rats and humans *in vivo* and *in vitro*. *Drug Metab. Dispos.* **31**(5):580–588 (2003). doi:10.1124/dmd.31.5.580.